

# $W^+ W^- H$ production through bottom quarks fusion at hadron colliders

**Biswajit Das**

Institute of Physics, Bhubaneswar, India

DPF21, Florida State University, July 12, 2021

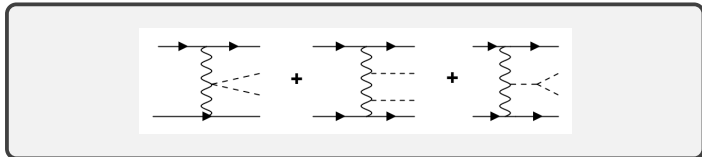


# Overview

- 1 Motivation
- 2 Diagrams
- 3 Coupling order
- 4 Amplitude Computation
- 5 Divergence issues
  - UV divergence
  - IR divergence
- 6 Results
  - SM prediction
  - Anomalous coupling effects
- 7 Summary

# Motivation : $b \bar{b} \longrightarrow W^+ W^- H$

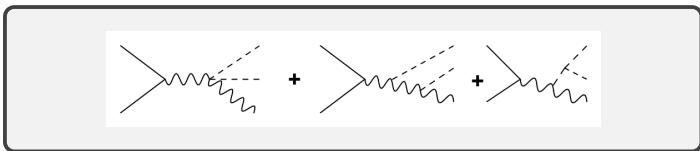
- Higgs sector in SM is not well explored, in particular  $HHH$ ,  $HHHH$  and  $VVHH$  couplings are still not well measured.
- Few processes can probe the  $VVHH$  coupling.
  - VBF mechanism for HH production



At HL-LHC the bound could be  $-0.43 < \kappa_{V_2 H_2} < 2.56$  at 95% confidence level. But the bound comes from both coupling  $WWHH$  and  $ZZHH$ .

# Motivation

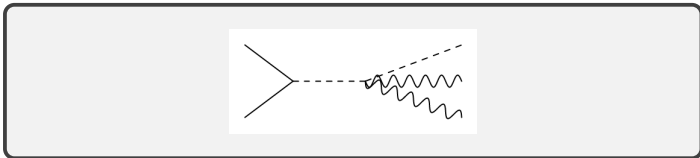
- Higgs-strahlung : HHV (V=W, Z) production



At the HL-LHC the bound will be quite weak

$$-10.6 < \kappa_{V_2 H_2} < 11.$$

- VVH (V=W, Z) production



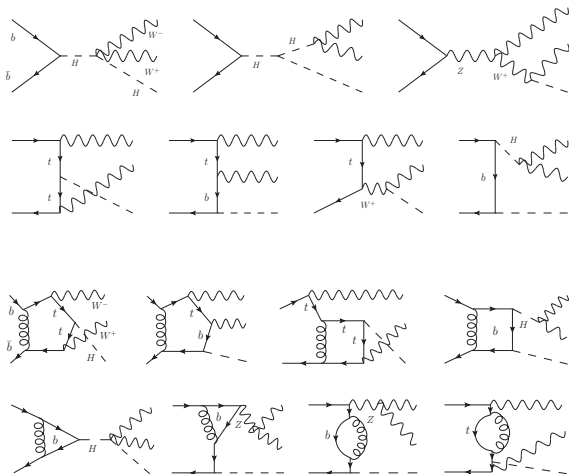
We can probe two  $VVHH$  couplings separately.

# Motivation

$pp \rightarrow WWH(\text{LO})$	$gg$	$q\bar{q}$	$b\bar{b}$
$\sigma(fb)$ at 14TeV	0.29	8.66	0.25
$\sigma(fb)$ at 27TeV	1.34	23.0	1.31
$\sigma(fb)$ at 100TeV	17.4	126.8	20.6

- The  $b\bar{b}$  contribution is sizeable. One should probe it in QCD regime.
- One can study the polarization dependence of physical observables which will be very useful for background suppression.

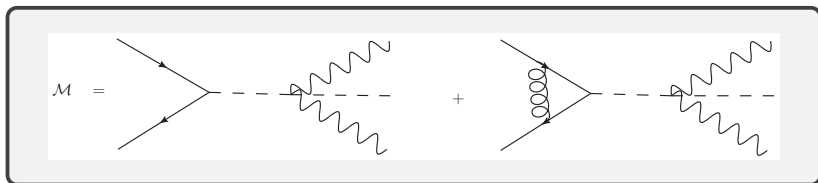
# Feynman diagrams :



# Feynman Diagrams :

- Total number of diagrams :
  - LO : 20 diagrams
  - NLO : Pentagon + Box + Triangle + Self Energy diagrams.  
Total 121 NLO diagrams.
- The trick is to calculate the minimum no. of diagrams, called *prototype diagrams* and then map the rest of the diagrams to those prototype diagrams.
  - LO prototype diagrams are 10
  - Loop-level prototype diagrams are 30.

# Coupling Order :



$$\mathcal{M} \sim g_w^3 \mathcal{M}_{LO} + g_s^2 g_w^3 \mathcal{M}_{NLO} + \mathcal{O}(g_s^4)$$

$$|\mathcal{M}|^2 \sim \alpha_w^3 |\mathcal{M}_{LO}|^2 + \alpha_s \alpha_w^3 \cdot 2\text{Re}(\mathcal{M}_{LO} \cdot \mathcal{M}_{NLO}^*) + \mathcal{O}(\alpha_s^2)$$

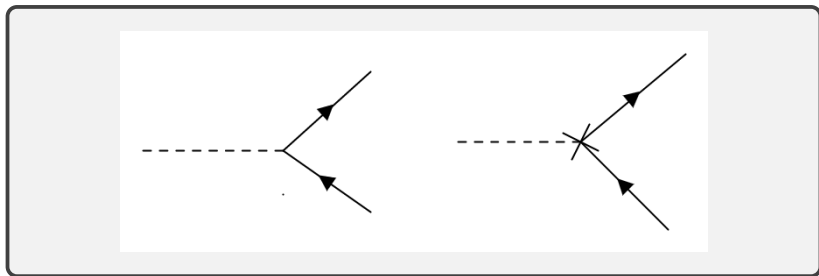


# Techniques to compute amplitudes :

- We compute helicity amplitudes by using spinor helicity formalism at the matrix element level.
- We use four-dimensional helicity (FDH) scheme to compute the amplitudes where all the  $\gamma$ -matrices, momentums and spinors are taken in 4-dimensions.
- In one-loop amplitude, individual one-loop Feynman diagram will give rise to tensor integrals containing powers of the loop momentum in the numerator.
- We use an in-house routine *OVReduce*, based on Oldenborgh-Vermaseren reduction techniques to reduce tensor integrals in terms of scalar integrals.
- We use the 'OneLOop' package for scalar integrals computation.

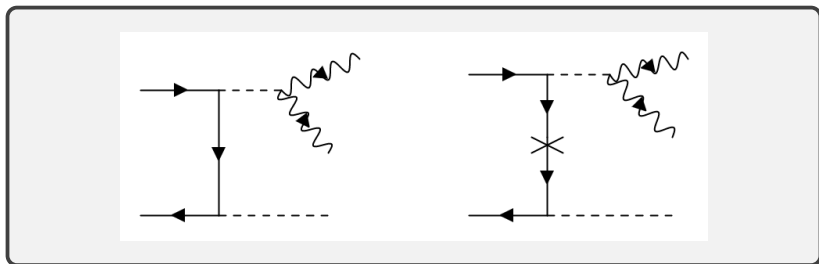
# UV divergence : Vertex CT diagrams

- QCD renormalizes the fermion mass.
- Higgs vertex will be renormalized due to mass involved in coupling.



- The Coupling strength of  $Hf\bar{f}$  vertex is  $-\frac{ig}{2} \frac{m_f}{m_W}$ .
- Counterterm for  $Hf\bar{f}$  vertex is  $-\frac{ig}{2} \frac{\delta m_f}{m_W}$ . Where  $\delta m_f = -\frac{\alpha_s}{4\pi} C_F \frac{6}{\epsilon}$ .

# UV divergence : Self-energy CT diagrams



- Counterterm for self energy diagram :  $-i(\not{p}\delta Z_2 - m_f\delta Z_m)$
- $\delta Z_2 = -\frac{\alpha_s}{4\pi} C_F \frac{2}{\epsilon}$  and  $\delta Z_m = -\frac{\alpha_s}{4\pi} C_F \frac{8}{\epsilon}$ .

# Infrared divergence :

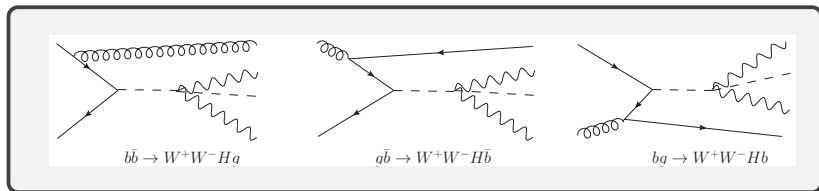
- IR or "mass singularities" arises from two kinds of singularities called the *collinear* and *soft* singularity. Singularities appear as  $\sim \ln(m/Q)$ . where  $m$  is the mass of the particle and  $Q$  is a large scale.

For the massless case

$$\sim 1/\epsilon, 1/\epsilon^2 \quad [\epsilon = (4 - D)/2]$$

- Because of light quarks and gauge bosons, most of the one-loop diagrams are IR singular.
- The real emission diagrams are also IR singular in soft and collinear regimes.
- The real emission and renormalized virtual amplitudes are both divergent in 4-dimension, but the sum of these two is finite.
- Three real emission sub-process can contribute to  $\sigma^{NLO}$ .  
 1.  $b\bar{b} \rightarrow W^+W^-Hg$ , 2.  $g\bar{b} \rightarrow W^+W^-H\bar{b}$  and 3.  
 $bg \rightarrow W^+W^-Hb$

# Subtraction scheme



- The real emission sub-processes starting with gluon have  $t$ -quark resonant diagrams which jeopardize the perturbative computations.
- We use  $b$ -quark tagging with 100% efficiency. We exclude these two sub-processes to avoid the  $t$ -quark resonances.
- We implemented the Catani-Saymour dipole subtraction method to remove IR singularities. The  $I$ -term exactly cancel the IR singularities in virtual diagrams and dipole terms  $\mathcal{D}_{ij,k}$  exactly cancel IR singularities in real emission diagrams.

# Results : SM predictions

We took SM parameters from PDG 2016. We use CT14lo and CT14nlo PDF set for LO and NLO cross section calculation respectively. We take  $\overline{MS}$  and On-shell renormalization scheme for massless and massive fermions respectively. The following results are in the ab unit for different CMEs with the scale uncertainties.

TeV	$\sigma_0(\alpha_w^3)$	$\sigma_{qcd}^{NLO}(\alpha_s\alpha_w^3)$	RE
14	$217^{+16.1\%}_{-18.9\%}$	$289^{+17.6\%}_{-20.8}$	33.2%
27	$1086^{+19.2\%}_{-20.5}$	$1559^{+18.0\%}_{-20.8}$	43.6%
100	$15258^{+22.0\%}_{-20.9\%}$	$23097^{+20.6\%}_{-21.0\%}$	51.4%

The relative enhancement is defined as  $RE = \left(\frac{\sigma_{qcd}^{NLO} - \sigma_0}{\sigma_0}\right)$ . We choose a dynamical scale as

$$\mu_R = \mu_F = \mu_0 = \frac{1}{3} \left( \sqrt{p_{T,W^+}^2 + M_W^2} + \sqrt{p_{T,W^-}^2 + M_W^2} + \sqrt{p_{T,H}^2 + M_H^2} \right)$$

# Results : SM predictions

Polarization dependence of cross section :

Pol. ( $W^+ W^-$ )	14 TeV (ab)			100 TeV (ab)		
	$\sigma_0$	$\sigma_{qcd}^{NLO}$	RE(%)	$\sigma_0$	$\sigma_{qcd}^{NLO}$	RE(%)
++	13	18	38.5	702	1056	50.4
+-	18	25	38.9	965	1499	55.3
+0	37	49	32.4	2568	3336	29.9
-+	4	6	50.0	229	334	45.9
--	13	18	38.5	707	1044	47.7
-0	22	28	27.3	1454	1346	-7.4
0+	22	28	27.3	1470	1216	-17.3
0-	37	49	32.4	2583	3151	22.0
00	51	67	31.4	4490	9748	117.1
$\sum$	217	289	32.2	15258	23097	51.4

Where  $+$   $\equiv \frac{1}{\sqrt{2}}(\epsilon_x + i\epsilon_y)$ ,  $-$   $\equiv \frac{1}{\sqrt{2}}(\epsilon_x - i\epsilon_y)$  and  $0 \equiv \epsilon_z$ .

Here we can see that there are huge contributions and increments in '00' polarization mode.

SM prediction

# $p_T$ -distributions :

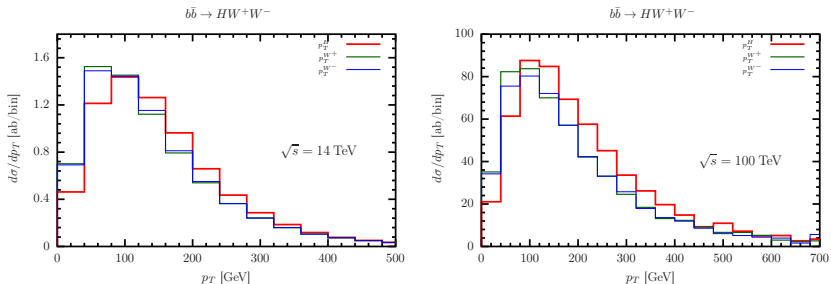


**Figure:** The NLO differential cross section distribution with respect to transverse momentums ( $p_T$ ) for 14 and 100 TeV CMEs.





# Differential distributions :

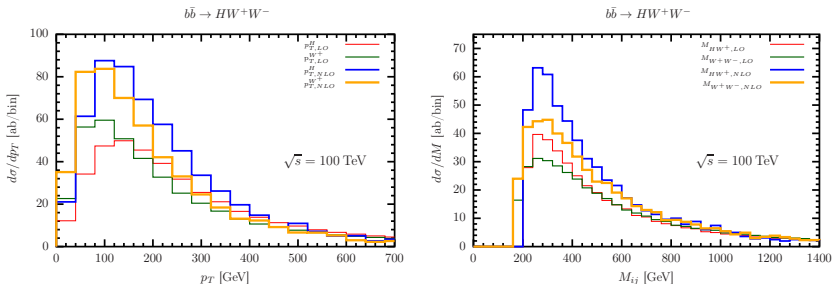


**Figure:** The LO and NLO differential cross section distribution with respect to transverse momentums ( $p_T$ ) and invariant masses ( $M_{ij/ijk}$ ) for 100 TeV CME.

# Differential distributions :

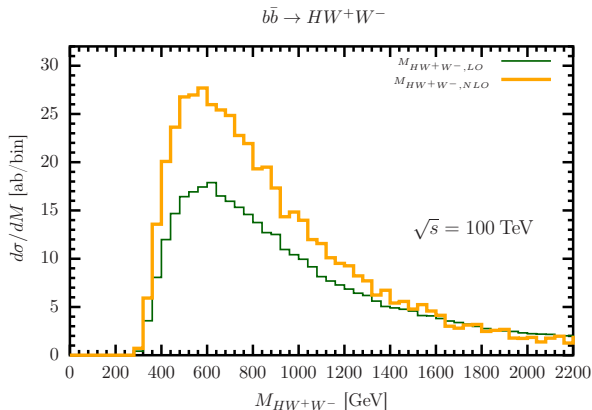


**Figure:** The LO and NLO differential cross section distribution with respect to invariant masses ( $M_{WWH}$ ) for 100 TeV CME.

# Anomalous coupling effects : $\kappa$ -framework

CME(TeV)	$\kappa_{V_2 H_2}$	$\sigma^{LO}$ [ab]	RI	$\sigma^{NLO}$ [ab]	RI
14	1.0 (SM)	217		289	
	2.0	216	[-0.5%]	288	[-0.3%]
	-2.0	222	[+2.3%]	295	[+2.1%]
100	1.0(SM)	15258		23097	
	2.0	14925	[-2.2%]	22607	[-2.1%]
	-2.0	16997	[+11.4%]	25465	[+10.3%]

**Table:** Effect of anomalous  $WWHH$  coupling on the total cross section at 14 and 100 TeV CMEs. Where  $RI = \frac{\sigma_{\kappa V_2 H_2} - \sigma_{SM}}{\sigma_{SM}}$ .

$\kappa_{V_2 H_2}$	$\sigma^{LO}$ [ab]	RI	$\sigma^{NLO}$ [ab]	RI
1.0 (SM)	4490		9748	
2.0	4159	[-7.4%]	9544	[-2.1%]
-2.0	6164	[+37.2%]	11993	[+23.0%]

**Table:** Effect of anomalous  $VVHH$  coupling in '00' mode at 100 TeV CME.



## Anomalous coupling effects

## Differential distributions :

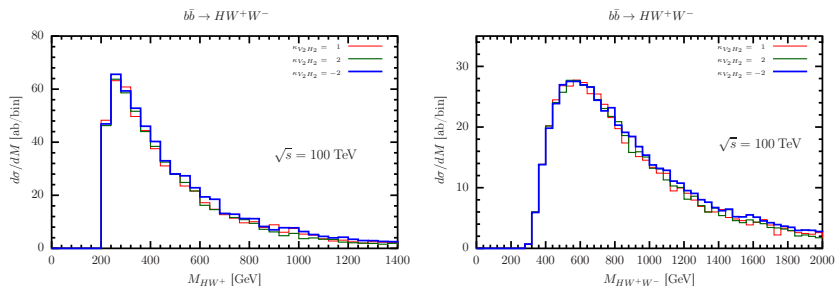


**Figure:** Effect of anomalous  $VVHH$  coupling on the differential cross section distribution at 100 TeV CME.

# Summary

- We have focused on the NLO QCD correction to  $b\bar{b} \rightarrow W^+W^-H$ . This process has significant dependence on  $VVHH$  coupling.
- The contribution of this process to  $pp \rightarrow W^+W^-H$  is only about 10 – 15% of that light quark scattering. But when both  $W$ -bosons are longitudinally polarized then this fraction can increase to 50%.
- At 100 TeV the NLO corrections are about 50% but the corrections are about 115%, when both  $W$ -bosons are longitudinally polarized.
- Our study suggests that the measurement of the polarization of the final state  $W/Z$ -bosons can be a useful tool to measure the couplings of the vector bosons and Higgs boson.
- Total cross section enhanced by 10% and cross section in '00' mode enhanced by 20 – 30% when we set  $\kappa_{V_2H_2} = -2$ .
- We find that the invariant mass and the  $p_T$  distributions are considerably harder for the negative values of  $\kappa_{V_2H_2}$ . This can also be useful to put a stronger bound on the coupling.

